# Relation between Rotational and Translational Dynamic Heterogeneities in Water

Marco G. Mazza,[1] Nicolas Giovambattista,[2,1] Francis W. Starr,[3] and H. Eugene Stanley[1]

[1]*Center for Polymer Studies and Department of Physics, Boston University, Boston, Massachusetts 02215, USA*
[2]*Department of Chemical Engineering, Princeton University, Princeton, New Jersey 08544-5263, USA*
[3]*Department of Physics, Wesleyan University, Middletown, Connecticut 06459, USA*

(Received 27 July 2005; published 9 February 2006)

We use molecular dynamics simulations to probe the rotational dynamics of the extended simple point charge model of water for a range of temperatures down to 200 K, 6 K above the mode coupling temperature. We find that rotational dynamics is spatially heterogeneous; i.e., there are clusters of molecules that rotate significantly more than the average for a given time interval, and we study the size and the temporal behavior of these clusters. We find that the position of a rotational heterogeneity is strongly correlated with the position of a translational heterogeneity, and that the fraction of molecules belonging to both kinds of heterogeneities increases with decreasing temperature. We further find that although the two types of heterogeneities are not identical, they are related to the same physical picture.

DOI: 10.1103/PhysRevLett.96.057803 PACS numbers: 61.20.Ja, 61.20.Gy

Experiments and computer simulations have shown that dynamics in supercooled liquids is spatially heterogeneous; i.e., one can identify transient regions with relaxation times different by orders of magnitude [1]. Simulations have shown that the most mobile particles tend to form clusters [2,3]. Different theoretical approaches have been developed to understand spatially heterogeneous dynamics [4,5]. In particular, Adam and Gibbs (AG) [4] postulate the existence of cooperatively rearranging regions (CRR) whose molecules change configuration independently of the rest of the system. Molecular dynamics (MD) simulations [6,7] have verified many of the predictions of the AG theory.

While there have been numerous studies of the heterogeneous nature of the translational degrees of freedom (TDOF) in water, there are few studies of the heterogeneous nature of the rotational degrees of freedom (RDOF). Here we systematically study the rotational dynamics of water and compare with the translational dynamics. Previous work for other systems suggests that translationally mobile molecules may have enhanced rotational mobility [8,9], and the characteristic times for the RDOF are smaller than for the TDOF [10]. To this end we perform MD simulations of a system of $N = 1728$ water molecules interacting with the extended simple point charge potential (SPC/E) for a range of temperatures from 350 K down to 200 K at the fixed density of 1 $\mathrm{g/cm^3}$; for each temperature we run two independent trajectories to improve the statistics [11,12].

We first quantify the rotation of a molecule using the normalized polarization vector $\hat{p}_i(t)$, defined as the normalized vector from the center of mass of the water molecule to the midpoint of the line joining the two hydrogens. In a time interval $[t, t + \delta t]$, $\hat{p}_i(t)$ spans an angle $\delta\theta \equiv \cos^{-1}[\hat{p}_i(t) \cdot \hat{p}_i(t + \delta t)]$. We define a vector $\delta\vec{\varphi}_i(t)$ such that $|\delta\vec{\varphi}_i(t)| = \delta\theta$ and its direction is given by $\hat{p}_i(t) \times \hat{p}_i(t + \delta t)$. Thus the vector $\vec{\varphi}_i(t) \equiv \int_0^t \delta\vec{\varphi}_i(t')dt'$ allows us to define a trajectory in a $\varphi$ space representing the rotational motion of molecule $i$. One can then associate a rotational mean square displacement (RMSD) given by

$$\langle\varphi^2(t)\rangle \equiv \frac{1}{N}\sum_i |\vec{\varphi}_i(t) - \vec{\varphi}_i(0)|^2 \tag{1}$$

and a rotational diffusion coefficient

$$D_R \equiv \lim_{t\to\infty} \frac{1}{4t}\langle\varphi^2(t)\rangle. \tag{2}$$

The vector $\vec{\varphi}_i(t)$ is not bounded to the unit sphere, since otherwise Eq. (2) would give $D_R = 0$. Equations (1) and (2) were applied in [14] to study a linear molecular system. If water molecules were linear, this one angle would suffice to fully describe the motion. To account for the fact that water molecules are not linear, we consider rotations also of the other two normalized principal vectors, which we label $\hat{q}_i(t)$ and $\hat{r}_i(t)$; we replace $\hat{p}_i(t)$ in the definition of $\vec{\varphi}_i$ with $\hat{q}_i(t)$ and $\hat{r}_i(t)$.

Figures 1(a) and 1(b) show the RMSD considering only the vector $\hat{p}$ (similar results hold for $\hat{q}$ and $\hat{r}$) and the temperature dependence of $D_R$ for all the three vectors, which we label $D_{R,p}$, $D_{R,q}$, and $D_{R,r}$. Similar to Ref. [14] we observe: (i) the RMSD shows three different regimes: a *ballistic* regime, where $\langle\varphi^2\rangle \propto t^2$, a plateau or *cage* regime, where molecules find themselves trapped in the cage formed by their neighboring molecules, and finally a *diffusive* regime where $\langle\varphi^2\rangle \propto t$; these three regimes are analogous to those observed in studies of translational dynamics of supercooled liquids. (ii) $D_R$ increases with $T$ with a non-Arrhenius behavior. While the values of $D_{R,p}$, $D_{R,q}$ and $D_{R,r}$ differ [as found in [13] ], they all show the same non-Arrhenius dependence on temperature. Note the oscillations in Fig. 1(a) present for times of the order of $10^{-2}$ ps. These oscillations, not present for linear molecules [14], correspond to the *libration* (hindered rotation)

 

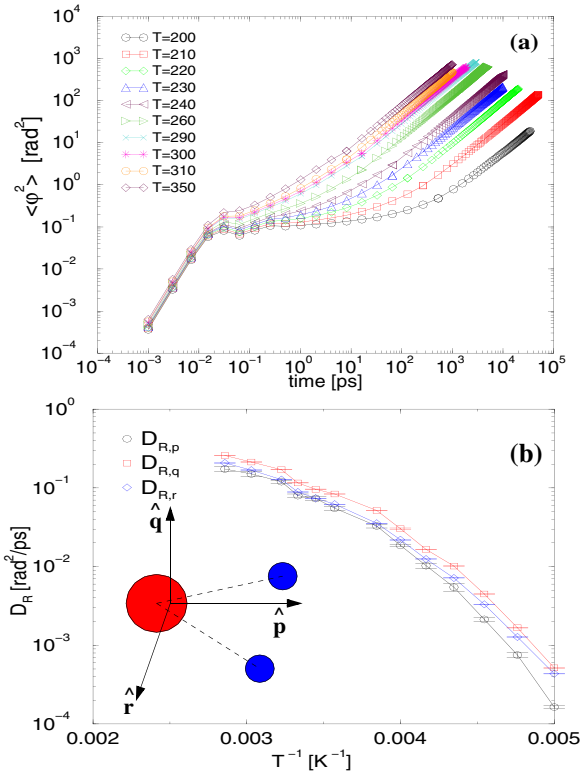


FIG. 1 (color online). (a) RMSD for rotations of the polarization vector, $\hat{p}$, in a range of temperatures from 200 to 350 K. (b) Rotational diffusivity, $D_R$, as a function of $T^{-1}$ for all three principal vectors, $\hat{p}$, $\hat{q}$, and $\hat{r}$. The inset shows a schematic defining these vectors ($\hat{p}$ is parallel to the dipolar moment of the molecule, $\hat{r}$ is parallel the hydrogen-hydrogen direction, and $\hat{q}$ is perpendicular to both $\hat{p}$ and $\hat{r}$).

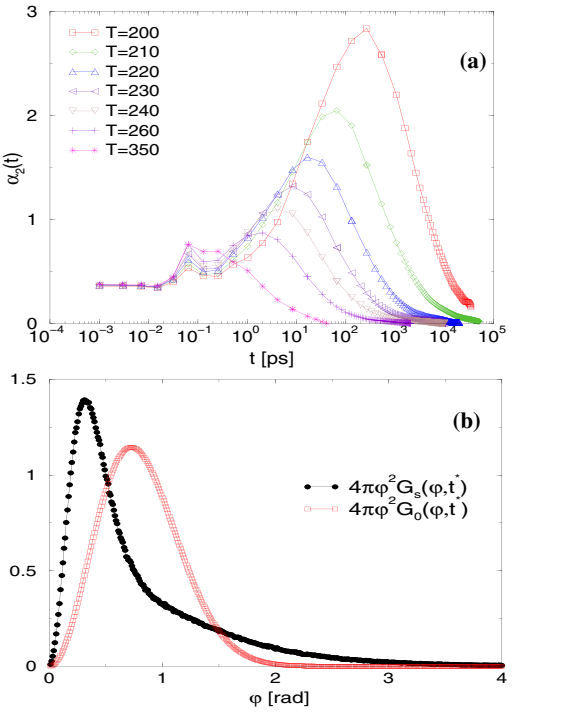


FIG. 2 (color online). (a) Non-Gaussian parameter $\alpha_2(t)$ for the range of temperatures indicated. (b) Self-part of the van Hove distribution function, $G_s(\varphi, t)$, for T = 200 K and $t^*(200\ \mathrm{K}) \approx 1.05$ ps, compared with the Gaussian approximation, $G_0(\varphi, t)$, obtained using $\langle\varphi^2(t^*)\rangle$ also at T = 200 K.

regime and occur at the same time as the oscillations observed in the rotational correlation function of water in [15].

We introduce the rotational counterpart of the self-part of the time-dependent van Hove distribution function, $G_s(\varphi, t)$ [16],

$$G_s(\varphi, t) \equiv \left\langle \frac{1}{N} \sum_{i=1}^{N} \delta(|\vec{\varphi}_i(t) - \vec{\varphi}_i(0)| - \varphi) \right\rangle, \qquad (3)$$

where $\langle \cdots \rangle$ represents average over configurations. With this formalism we recover the usual interpretation for $4\pi\varphi^2 G_s(\varphi, t)$ as the probability of having a molecule at time $t$ with angular displacement $\varphi$. In other words, that in the abstract $\varphi$ space, a molecule has moved to a distance $\varphi$ from its position at $t = 0$. For long times the diffusion equation for $\vec{\varphi}_i(t)$ holds, and $G_s(\varphi, t)$ is a Gaussian distribution

$$G_0(\varphi, t) = \left[\frac{3}{2\pi\langle\varphi^2(t)\rangle}\right]^{3/2} \exp[-3\varphi^2/2\langle\varphi^2(t)\rangle]. \qquad (4)$$

The deviations of $G_s(\varphi, t)$ from $G_0(\varphi, t)$ can be quantified by the non-Gaussian parameter [17] $\alpha_2(t) \equiv 3\langle\varphi^4(t)\rangle / 5\langle\varphi^2(t)\rangle^2 - 1$. Figure 2(a) shows $\alpha_2(t)$ for different temperatures. $\alpha_2(t)$ shows a clear maximum at $t = t^*(T)$ which corresponds to the beginning of the diffusive regime for the RDOF [Fig. 1(a)]. We note that there is a small maximum at $t \approx 10^{-2}$ ps: this is a consequence of the librational motion as shown in Fig. 1(a) [18]. By considering $t^*(T)$ we find that at all $T$ the diffusive regime occurs for the RDOF at a slightly earlier time than for the TDOF. Figure 2(b) shows $G_s(\varphi, t)$ and $G_0(\varphi, t)$ for $T = 200$ K and $t = t^*(200\ \mathrm{K}) \approx 1.05$ ns. As in [7] we find that $G_s(\varphi, t^*)$ and $G_0(\varphi, t^*)$ intersect for large $\varphi$ at $\varphi^*$, and $G_s(\varphi, t^*)$ shows a large tail where the fitted Gaussian underestimates the angular motion of the molecules. Molecules with $\varphi > \varphi^*$ can be considered with an angular displacement higher than expected; this fraction $f \equiv \int_{\varphi^*}^{\infty} 4\pi\varphi^2 G_s(\varphi, t)$ is found to be $\approx 13\%$, showing a weak $T$ dependence.

In analogy to [7,19,20], we define the rotational mobility of a molecule at a given time $t_0$ as the maximum angular displacement in the interval $[t_0, t_0 + \Delta t]$ of the oxygen atom

$$\Psi_i(t, \Delta t) \equiv \max\{|\vec{\varphi}_i(t + t_0) - \vec{\varphi}_i(t_0)|, t_0 \le t \le t_0 + \Delta t\}. \qquad (5)$$

We focus our attention on the most rotationally mobile molecules and explore the possibility that there exist clusters also among this category of molecules. To facilitate comparison with the study [7] of translational heterogene-

ities (TH), we select the 7% of the most rotationally mobile molecules [21] and define a cluster at time $t_0$ over an observation time $\Delta t$ as those molecules whose nearest neighbor oxygen-oxygen (O-O) distance at time $t_0$ is less than 0.315 nm (first minimum of O-O radial distribution function). We find that the rotational dynamics is spatially heterogeneous, since these molecules form clusters, which we will call rotational heterogeneities (RH). Furthermore, we obtain different clusters depending on which vector ($\hat{p}$, $\hat{q}$, or $\hat{r}$) we consider. We refer to these as $\hat{p}$, $\hat{q}$, or $\hat{r}$ clusters.

Next we address the question of how these RH depend on the observation time. The weight average cluster size is $\langle n(\Delta t)\rangle_w \equiv \langle n^2(\Delta t)\rangle/\langle n(\Delta t)\rangle$, where $\langle n(\Delta t)\rangle$ is the average number of molecules in a cluster in a time $\Delta t$. To eliminate the contribution of random clusters, we normalize $\langle n(\Delta t)\rangle_w$ by $\langle n_r\rangle_w$, i.e., the weight average cluster size obtained by choosing randomly 7% of the molecules. Figure 3 shows $\langle n(\Delta t)\rangle_w/\langle n_r\rangle_w$ for $\hat{p}$ clusters as a function of $\Delta t$ for different $T$ (similar results hold for $\hat{q}$ and $\hat{r}$). In the same manner as the translational case, the maximum in $\langle n(\Delta t)\rangle_w/\langle n_r\rangle_w$ occurs at the end of the cage regime of the RMSD, indicating that the cage breaking of the RDOF is highly correlated with the cage breaking of TDOF. The RH become larger as $T$ decreases. Figure 4(a) shows $\langle n(\Delta t)\rangle_w/\langle n_r\rangle_w$ for RH (obtained from $\hat{p}$, $\hat{q}$, or $\hat{r}$) and TH at the corresponding $t_{\max}$, the time at which the corresponding weight average cluster size is largest. We find that on average TH are larger than RH, and that RH reach their maximum size before the TH, Fig. 4(b); i.e., $t_{\max}$ for RH is smaller than $t_{\max}$ for TH.

It is natural to ask to what extent the RH and TH are formed by the same molecules. We address this question by simultaneously analyzing the properties of RH and TH. We considered the RH defined from $\hat{p}$, but the same physical picture holds when using $\hat{q}$ or $\hat{r}$. Figure 5(a) is a typical snapshot of the system, showing both TH and RH. The clusters together form a larger entity characterizing the dynamical heterogeneities; the molecules belonging to both kinds of clusters act as the "backbone" of such an entity. We find that the fraction $f_{\mathrm{RT}}$ of molecules simultaneously belonging to both clusters increases with decreasing temperature. Figure 5(b) shows $f_{\mathrm{RT}}$ at the lowest temperature simulated for the three kinds of RH. We observe that the maximum value of $f_{\mathrm{RT}}$ is 6% for the case of $\hat{p}$, while this value becomes 27% for $\hat{q}$ or $\hat{r}$. Thus the $\hat{q}$ and $\hat{r}$ clusters couple more strongly with the TH clusters.

To compare the structure of the TH and RH, we evaluate the radial distribution function (RDF) of oxygen atoms within each kind of cluster, and between the two kinds of clusters. Figure 5(c) shows the RDF for TH, for RH (defined from $\hat{p}$, but the same results are obtained by using $\hat{q}$ or $\hat{r}$), and for molecules which belong to *both* TH and RH. We see that there is a strong tendency for mobile molecules (of either type) to be neighbors. The RDF's are qualitatively similar to the bulk RDF, $g_{\mathrm{bulk}}(r)$, with maxima at $r \approx 0.28$ nm and $r \approx 0.45$ nm (i.e., molecules are nearest or next-nearest neighbors); however, the amplitudes of the first peak are strongly enhanced compared to bulk water. In order to examine deviations from the bulk we normalize the RDF's by $g_{\mathrm{bulk}}(r)$ [inset of Fig. 5(c)]. All of the RDF's display maxima at 0.32 nm, indicating that oxygens in TH and RH have an enhanced tendency (with respect to the bulk) to be in the first interstitial shells of each other and, therefore, have more than four nearest neighbors. Molecules with five or more neighbors have bifurcated

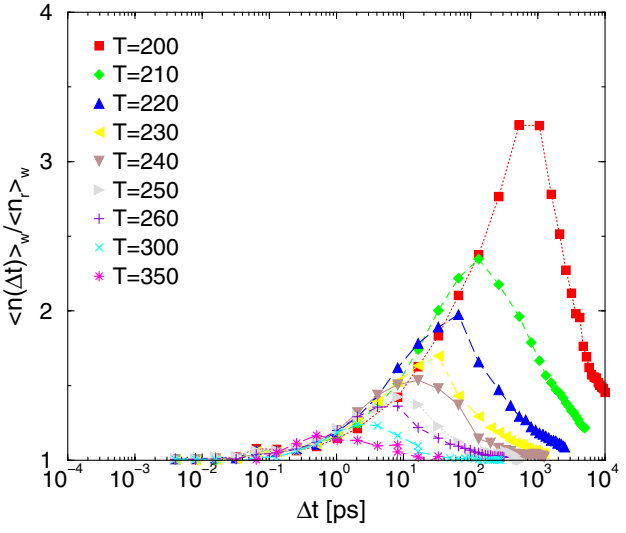


FIG. 3 (color online). Weight average cluster size for T = 200–350 K for molecules belonging to the 7% most rotationally mobile molecules. The values are normalized to the random cluster contribution.

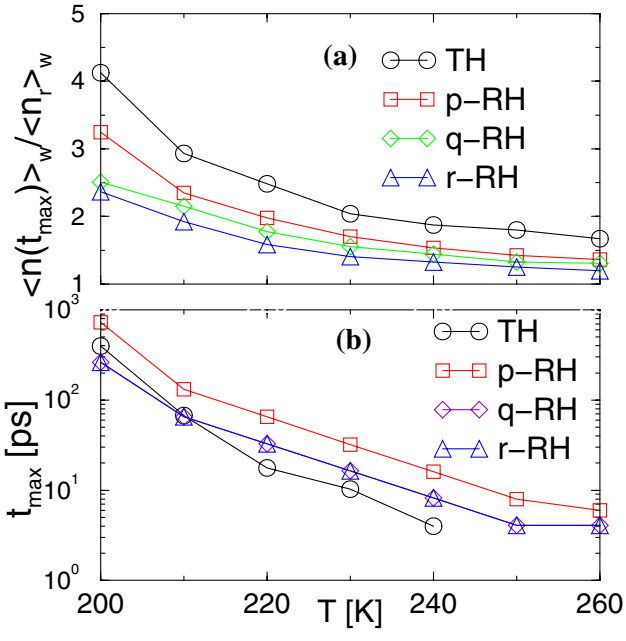


FIG. 4 (color online). (a) Weight average cluster size as a function of temperature for TH and RH. Both quantities are calculated at the corresponding $t_{\max}$. Note that the TH are larger than the RH. (b) The time $t_{\max}$ at which the maximum of the weight average cluster size occurs.

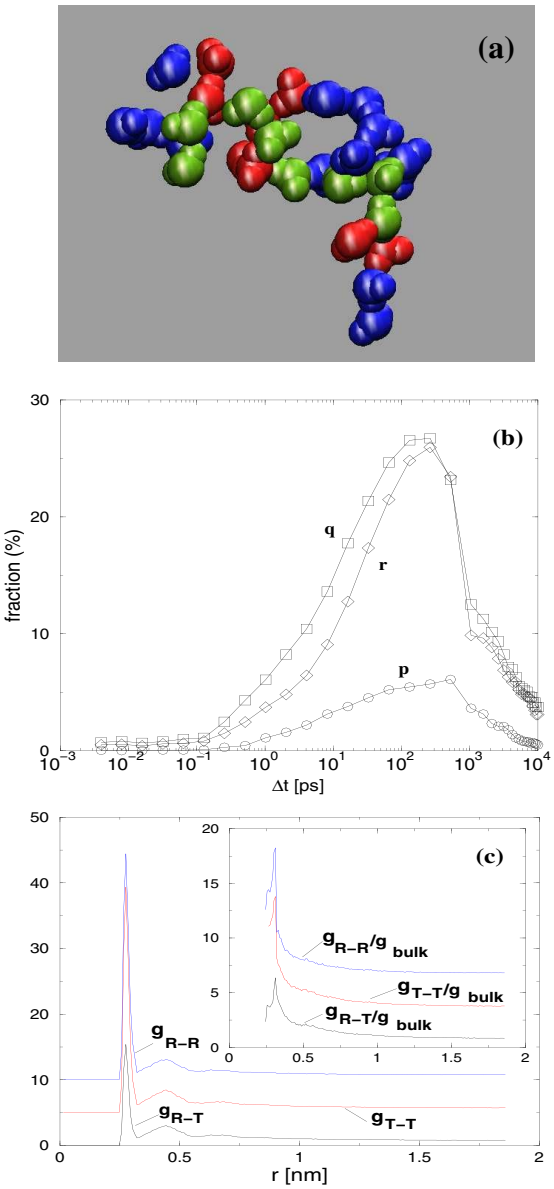


FIG. 5 (color online). (a) A snapshot of a typical cluster at T = 200 K. The red molecules belong to TH, blue to RH, and the green molecules belong to both clusters. (b) Fraction of molecules in both a TH and RH for the three principal vectors; the strongest correlations are for vectors $\hat{q}$ and $\hat{r}$. (c) RDF between the sets of translationally mobile and rotationally mobile molecules for T = 200 K. The inset shows the corresponding ratios of these functions to $g_{\mathrm{bulk}}(r)$. For clarity $g_{\mathrm{T-T}}$ is shifted by 5 and $g_{\mathrm{R-R}}$ by 10 on the vertical axis; the ratio involving $g_{\mathrm{T-T}}$ is shifted by 3 and the ratio involving $g_{\mathrm{R-R}}$ by 6 in the inset.

bonds and represent ''defects'' in the tetrahedral network characterizing water [22,23]. Therefore, our results suggest that the combined TH and RH in water (i) are a consequence of the defects of the HB network [24] and (ii) are primarily composed by molecules located at the defects of the HB network: evidence of the relation between the structure and dynamics in water. Thus the physical picture needed to describe rotational heterogeneities resembles that needed for describing translational heterogeneities.

We thank the Collaborative Research in Chemistry program of NSF (CHE-0404673), the Computational Chemistry Program (CHE 0096892) for support, and the Boston University Computation Center for a generous allocation of CPU time.

[1] H. Sillescu, J. Non-Cryst. Solids **243**, 81 (1999); M. D. Ediger, Annu. Rev. Phys. Chem. **51**, 99 (2000); I. Ohmine and H. Tanaka, Chem. Rev. **93**, 2545 (1993); S. C. Glotzer, J. Non-Cryst. Solids **274**, 342 (2000), and references therein; R. Richert, J. Phys. Condens. Matter **14**, R703 (2002).
[2] C. Donati *et al.*, Phys. Rev. Lett. **80**, 2338 (1998).
[3] D. N. Perera and P. Harrowell, J. Non-Cryst. Solids **235**, 314 (1998).
[4] G. Adam and J. H. Gibbs, J. Chem. Phys. **43**, 139 (1965).
[5] J. P. Garrahan and D. Chandler, Phys. Rev. Lett. **89**, 035704 (2002).
[6] A. Scala *et al.*, Nature (London) **406**, 166 (2000).
[7] N. Giovambattista *et al.*, Phys. Rev. Lett. **90**, 085506 (2003); Phys. Rev. E **72**, 011202 (2005).
[8] J. Kim and T. J. Keyes, Chem. Phys. **121**, 4237 (2004).
[9] M. C. C. Ribeiro, Phys. Chem. Chem. Phys. **6**, 771 (2004).
[10] G. Matsui and S. Kojima, Phys. Lett. A **293**, 156 (2002).
[11] Simulation details are given in: F. W. Starr *et al.*, Phys. Rev. E **60**, 6757 (1999).
[12] Note that classical simulations cannot capture any perturbation in the dynamics due to quantum effects, as discussed in [13].
[13] I. M. Svishchev and P. G. Kusalik, J. Phys. Chem. **98**, 728 (1994); L. H. de la Pena and P. G. Kusalik, J. Am. Chem. Soc. **127**, 5246 (2005).
[14] S. Kammerer *et al.*, Phys. Rev. E **58**, 2141 (1998).
[15] L. Fabbian *et al.*, J. Non-Cryst. Solids **235**, 325 (1998).
[16] J. P. Hansen and I. R. McDonald, *Theory of Simple Liquids* (Academic, New York, 1986).
[17] A. Rahman, Phys. Rev. A **136**, A405 (1964); K. Skold *et al.*, *ibid.* **6**, 1107 (1972).
[18] Note that for $t \to 0$, contrary to [7] for TDOF, $\alpha_2(t \to 0) \approx 0.37$. This value of $\alpha_2$ can be obtained analytically from a Boltzmann distribution of a free rotator and noting that for short times $\vec{\varphi}_i(t) \simeq \vec{\omega}_i(t)\delta t$, where $\vec{\omega}_i$ is the angular velocity for the $i$th molecule.
[19] C. Donati *et al.*, Phys. Rev. E **60**, 3107 (1999).
[20] E. R. Weeks *et al.*, Science **287**, 627 (2000).
[21] Our results are not qualitatively affected by the choice of $f$, provided $f \lesssim 15\%$.
[22] L. Fabbian *et al.*, Phys. Rev. E **60**, 5768 (1999), and references therein.
[23] L. Bosio *et al.*, Phys. Rev. A **27**, 1468 (1983).
[24] These results are consistent with F. Sciortino, A. Geiger, and H. E. Stanley, Nature (London) **354**, 218 (1991); J. Chem. Phys. **96**, 3857 (1992), where an enhanced translational diffusivity was found for molecules with more than four neighbors.